Effect of Increased Water-Based Adhesive Content with Portland Cement on the Curing Performance of Structural Biofiber Cement Board Composites from Recycled Cement Packaging Bags via Uniaxial Pressing

Nuchnapa Tangboriboon * and Panisara Panthongkaew

Posted Date: 26 February 2026

doi: 10.20944/preprints202602.1693.v1

Keywords: structural composites; biofiber cement boards; portland cement; thermal insulation materials

Article

Effect of Increased Water-Based Adhesive Content with Portland Cement on the Curing Performance of Structural Biofiber Cement Board Composites from Recycled Cement Packaging Bags via Uniaxial Pressing

Nuchnapa Tangboriboon * and Panisara Panthongkaew

The Materials Engineering Department, Faculty of Engineering, Kasetsart University, Bangkok 10900, Thailand
* Correspondence: fengnnpt@ku.ac.th; Tel. 66-2-797-0999-2106; Fax. 66-2-955-1811

Abstract

This research explores the development of high-strength biofiber cement boards with good thermal insulation, using recycled biofiber derived from cement packaging combined with a water-based adhesive and Portland cement through a cementation-curing process. This approach reduces cement packaging and other biofiber waste, promoting environmental sustainability without requiring chemical additives or incineration of waste biofibers. Recycled biofiber from cement bags, composed primarily of cellulose (60 wt%), lignin (15 wt%), and hemicellulose (10 wt%), serves as a reinforcing phase, while the cement and adhesive mixture provide a strong binding matrix. The physical, mechanical, chemical, and thermal properties of the biofiber cement boards were evaluated in accordance with relevant industrial standards, including TISI 878:2023, BS 874, ASTM D570, ASTM C518, ISO 8301, and JIS A1412. The findings show that a higher ratio of water-based adhesive to cement mortar (1:2), combined with a higher content of biofiber sheets, significantly enhances performance, particularly in Formulas 7, 8, and 9. The resulting boards demonstrate strong bonding ability, improved fire resistance, better moisture and weather resistance, and longer service life compared to lower ratios. These outcomes highlight the potential of recycled biofiber composites as sustainable alternatives for thermal insulation and structural applications, such as ceilings and walls in building construction.

Keywords: structural composites; biofiber cement boards; portland cement; thermal insulation materials

1. Introduction

The expansion of the infrastructure sector is a major driver of global cement demand. Urbanization has increased the need for residential, commercial, and transport infrastructure, including roads, bridges, and airports, which in turn drives cement consumption and creates a growing demand for efficient packaging. Companies are increasingly investing in biodegradable, recyclable, and paper-based packaging, including 20 kg, 40 kg, and 50 kg bags, to meet local construction needs while supporting sustainability goals. The rise of small-scale construction projects has further fueled demand for more portable packaging solutions. Advances in cement technology have introduced environmentally friendly alternatives, such as Portland cement, mortar cement, blended cement, and geopolymer cement incorporating slag, fly ash, or natural pozzolans. These alternatives reduce carbon emissions and increase the need for diverse and high-volume packaging solutions. Packaging processes have also improved through automation, robotics, and innovative materials, enhancing efficiency, reducing costs, and meeting growing demand. Consumer interest in eco-friendly products, coupled with regulatory requirements, has driven the

 doi:10.20944/preprints202602.1693.v1

adoption of recyclable, biodegradable, and reusable packaging. However, because cement is highly sensitive to moisture, which can cause premature hardening and reduce product quality, developing moisture-resistant packaging remains a challenge. Traditional non-recyclable plastic packaging also poses environmental concerns, prompting a shift toward sustainable solutions. Eco-friendly paper-based packaging is increasingly preferred for its strength, recyclability, and ease of branding.

Globally, cement production contributes approximately 8% of CO_2 emissions, potentially rising to 3.8 billion tons annually, placing additional pressure on the industry to adopt sustainable practices. Paper-based packaging is expected to grow steadily due to its sufficient strength for transporting cement, ease of recycling, and compatibility with branding. Biofiber-based cement bags protect cement from moisture and contaminants, reduce spoilage, and can be customized for branding, ensuring safe and efficient transport while supporting market growth. However, discarded cement packaging contributes to environmental waste and can harbor microorganisms. This has led to efforts to recycle cement packaging for industrial production, transforming used bags into building materials such as ceiling panels and lightweight gypsum walls. Incorporating additives and bonding enhancers improves adhesion, while accelerated heat curing increases strength, reduces water absorption, enhances heat resistance, and facilitates installation. These recycled products can also be integrated into buildings and finished with paint, tiles, or other decorative materials. In parallel, hundreds of tons of wastepaper are collected daily from offices and households, much of which is either incinerated or sent to landfills, contributing to environmental pollution. The most sustainable approach is to reduce, reuse, and recycle wastepaper and biofiber. Waste biofiber, such as newspapers and cement packaging, is primarily composed of 60 wt% cellulose, 15 wt% lignin, 10 wt% hemicellulose, and other additives [1,2]. Recycling such biofiber can reduce energy and water consumption by up to 70%, lower greenhouse gas emissions, conserve forests, and decrease landfill contributions, as illustrated in Scheme 1. Additionally, recycling provides a sustainable method for producing innovative products, reduces the demand for new raw materials, and limits emissions of methane and other toxic gases, which are more harmful than CO_2 [3,4]. Since biofiber production traditionally relies on wood, timber, and hydrocarbons, recycling newspapers and cement packaging also helps conserve these resources. As a biodegradable, cellulose-based material, biofiber from cement packaging have significant potential in industries such as construction, composites, packaging, petrochemicals, and catalysis [5–8]. Repurposing waste cement packaging into new products reduces environmental impact while alleviating pressure on raw material supplies. Advances in utilizing recycled biofibers include studies by Mazaherifar et al., who developed foam composites from recycled cardboard using corn starch as a binder, demonstrating potential for insulation applications [9]. Similarly, Jensen et al. created cost-effective insulation panels from recycled lignocellulosic waste, including glass powder, plastic, rice husk, and wastepaper— with favorable thermal performance [10]. Bayatkashkoli et al. investigated high-pressure laminates made from recycled paper and newspapers using phenol-formaldehyde resins and borax as reinforcement [11]. Ferreira et al. developed multifunctional electronic paper (e-paper) from recycled newspapers for smart applications like energy harvesters and pressure sensors [12]. Recycled biofibers are also used in industries such as construction [13], electronics and sensors [14,15], batteries [16–19], solar cells [20–22], supercapacitors [23,24], and medical technologies [25,26]. Producing composite materials and lightweight fiber cement boards from biofibers involves using adhesives to bond surfaces firmly and permanently, as shown in Scheme 2. The adhesive-adherent interface typically relies on secondary bonds like van der Waals and hydrogen bonds due to the chemical structure of the materials, as depicted in Scheme 3. Adhesives range from hydrophobic to hydrophilic and natural to synthetic types, including gelatin [25], starch, polyvinyl acetate (PVA) [25,26], urea-formaldehyde resins [27], epoxy resin [28], phenolic-formaldehyde resin [29–31], natural rubber [32], and cement [1,34]. Polyepoxides (epoxy resins) are well-known for their excellent adhesion, chemical and heat resistance, and mechanical properties such as high tensile, compressive, and

 doi:10.20944/preprints202602.1693.v1

bending strength. These resins are widely used in coatings, composites, electronics, and structural adhesives. Polyepoxy adhesives exhibit high shear strength, thermal and chemical resistance, and minimal shrinkage, making them ideal for encapsulating electronic components and protecting them from environmental damage.

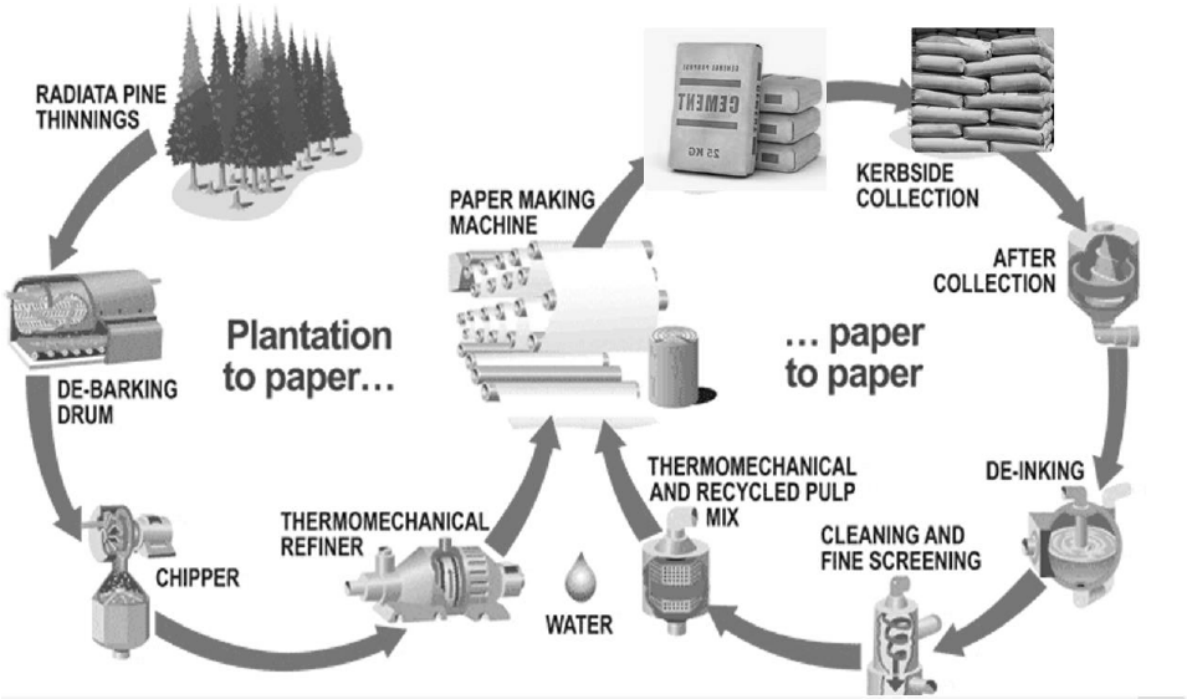

Scheme 1. Steps of biofiber manufacturing for industrial use.

Building materials	Thermal conductivity, at 300 K (W/m.K)	Bulk density (g/cm^3)	Compressive strength (MPa)	Bending strength (MPa)	Tensile strength (MPa)	Young's modulus of Elasticity (MPa)
Brick	0.70	2.50-2.80	126	2.15	1.50-2.88	11000
Plastered clay brick	0.81	1.75	3.5	3.63	0.72	56000
Red brick	0.50	1.70	10.29	0.015	2.80	14000
Cement	1.01	1.90	11.50-17.50	5.50	2.0-5.0	10000-30000
Concrete-cast dense	1.40	2.24-2.40	0.30-40.00	1.50-3.20	2-5	50000
Concrete-cast light	0.40	1.12-1.92	17.00	4.20	2.0	30000
Glass	1.05	2.20	1000	45-120	7.0	70000
Single glass window	0.65	2.50	4.14	26.90	1000	69000
Mineral wool	0.38	1.20-1.40	0.0029	13	26-50	830-1200
Mortar	0.80	1.90	11.50-17.50	1.03	1.70	2200
Plaster (Gypsum)	0.46	1.30	3-75	4.50	4.50	2989
Plasterboard (Gypsum)	0.16	0.60	4-8	2-4	1-2	4350
Polystyrene foam	0.032	1.05	039-10.9	0.075-3.00	31.0-41.4	1140-1550
Polyurethane foam	0.025	0.05-0.96	0.15-0.22	0.95-1.75	0.02-1900	15-152
Stone (Limestone)	1.30	1.19-1.49	13.8-255	1-10	5-25	55.1-82.7
Stone (Granite)	1.70-4.00	2.46-2.80	96.5-310	15-25	7-25	92.7
Timber (Softwood)	0.14	0.40-0.60	30-60	75	70-140	4141-6474
Timber (Hardwood)	0.14-0.17	0.61-0.67	10.89	151.20	51-120	11000-13000
Woodfiber board	0.11	0.25	1.20	50-250	15.2-20.7	4000
Fiberglass	0.05	2.10	90.38	10.36	4800	72000
Tile (Ceramics)	1.30	2.38-2.45	125-250	0.24	45-73	51000
Asphalt	0.70	2.20-2.40	3.6	0.031	0.69	2110
Steel	47.60	7.80-7.90	250-400	370-520	400-550	190000-215000
Marble	1.30	2.60-2.90	32.7-210	12-20	7-20	60000
Rubber	0.92-1.05	0.93	0.063	10-30	25	3

Scheme 2. Standard values for thermal conductivity, physical and mechanical property of building materials.

 doi:10.20944/preprints202602.1693.v1

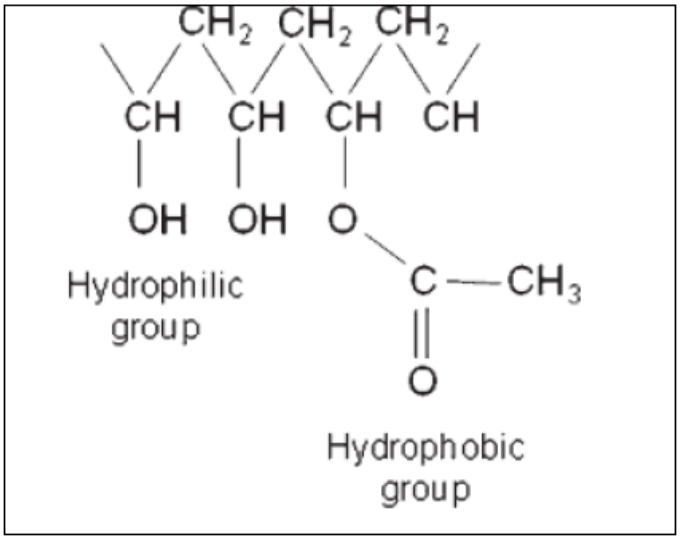

Scheme 3. Chemical formula of a water-based PVAc adhesive.

Cement, a widely used binding agent in construction, exhibits adhesive and cohesive properties. When mixed with water, it undergoes hydration and exothermic reactions, forming a solid state. The curing process improves the material's physical (e.g., appearance, color, density, setting time, shrinkage), mechanical (e.g., compressive, tensile, and flexural strength), and thermal (e.g., conductivity) properties as shown in Scheme 4a. However, using cement alone can result in excessive rigidity with low tensile strength. To improve flexibility and tensile performance, polymers are often incorporated. There are many types of water-based adhesives, such as polyvinyl alcohol (PVA, $[-CH_2-CH(OH)-]_n$), polyvinyl acetate (PVAc, $[-CH_2-CH(OCOCH_3)-]_n$), commonly known as "white glue," starch- or dextrin-based adhesives ($(C_6H_{10}O_5)_n$), and acrylic water-based adhesives ($[-CH_2-CH(COOC_2H_5)-]_n$). When water reacts with cement through hydration, several products are formed: calcium silicate hydrate (C-S-H gel), calcium hydroxide ($Ca(OH)_2$, or portlandite) from silicate hydration, and ettringite or monosulfate from aluminate reactions. For example, combining cement with water-based adhesives or polyvinyl alcohol enhances adhesion and tensile properties. Portland cement containing polyvinyl alcohol, at an optimal polyvinyl alcohol-to-cement ration of 3:7, demonstrates superior performance. Curing involves the formation of a three-dimensional polymeric network, which enhances durability and performance. Water-based epoxy adhesives are accelerated by the heat generated during cement hydration, eliminating the need for external stimuli such as UV radiation. This dual curing mechanism transforms the liquid solution into a solid product [35,36]. To achieve complete setting of the water-based adhesive, it is typically necessary to increase the process temperature after gelation. A straightforward method for monitoring changes in viscosity and the extent of the reaction during curing is by measuring the variation in the elastic modulus—specifically, the storage modulus (G′) and the loss modulus (G″). The evolution of G′ and G″ over time provides valuable insights into the progression of the curing reaction, as illustrated in Scheme 4b. Initially, during the induction phase, both G′ and G″ begin to rise, exhibiting a noticeable change in slope. At a specific point, the two moduli intersect; beyond this point, the rates of increase for G′ and G″ slow down, and the moduli eventually stabilizes at a plateau. Once the plateau is reached, the reaction is considered complete. The degree of curing starts at zero (at the beginning of the reaction) and progresses to one (upon reaction completion). The slope of the curve changes over time, reaching its maximum approximately halfway through the reaction, as shown in Scheme 2b. The degree of curing (α) can be calculated using the following equation:

 doi:10.20944/preprints202602.1693.v1

$$\alpha = \frac{G'(t) - G'_{min}}{G'_{max} - G'_{min}} \quad (1)$$

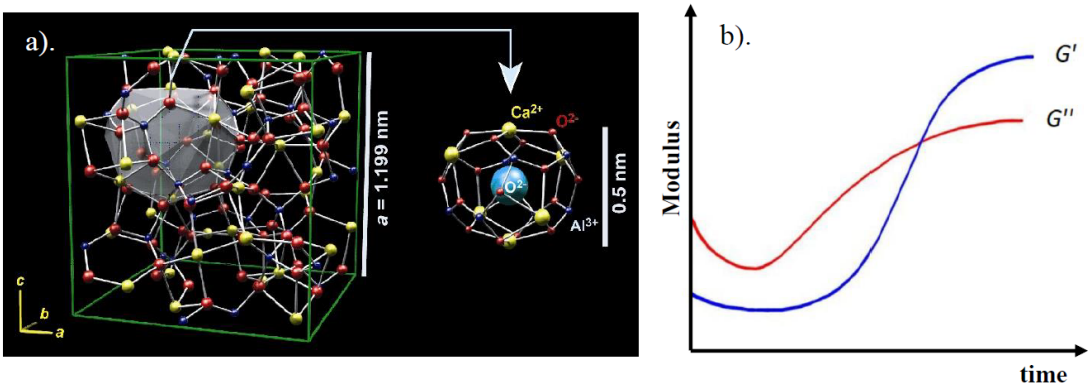

Scheme 4. a). Structure of mortar cement (calcium aluminate) powder and b) Evolution in time of storage modulus G′ and loss modulus G″ during a curing reaction.

During crosslinking, an exothermic reaction takes place, and the crosslinking rate is directly proportional to the heat released during the process. The greater the number of bonds formed; the more heat is released. Once the reaction is complete, no additional heat is generated. The degree of curing (α) can be expressed as:

$$\alpha = \frac{Q}{Q_T} = \frac{\int_0^s \dot{Q}\, dt}{\int_0^{s_f} \dot{Q}\, dt} \quad (2)$$

where Q represents the heat released up to a specific time s, $\dot{Q}$ s is the instantaneous rate of heat release, and Q_T is the total amount of heat released when the reaction is complete at time in s_f.

In this study, biofiber cement boards were fabricated as structural composites using a combination of polymer adhesive and Portland cement. Structural composites are engineered materials formed by combining two or more distinct components to achieve enhanced performance; in such systems, the collective properties exceed those of the individual constituents. Typically, a structural composite consists of two primary elements: a matrix—here composed of Portland cement and polymer adhesive—and a biofiber reinforcing phase. The matrix binds and protects the reinforcement, preventing deformation or fracture under stress, while the reinforcement provides strength and stiffness, which are the key contributors to the composite's mechanical performance. Structural composites are generally designed to withstand loads in specific directions and can be optimized for strength either along a single axis or across multiple directions. This work aims to develop biofiber cement board composites for decorative applications, ceiling panels, and wall insulation by utilizing recycled cement packaging as a biofiber reinforcement, combined with a water-based PVAc adhesive and Portland cement through a multilayer pressing process. As illustrated in Scheme 5, the cement packaging biofibers and PVAc adhesive were stacked and integrated with Portland cement to form the structural composite. The incorporation of cement with PVAc adhesive accelerates both the cement hydration and adhesive curing reactions, thereby improving setting behavior, mechanical strength, physical appearance, and thermal resistance, as shown in Scheme 2. The resulting composites were comprehensively characterized. Mechanical properties, including tensile strength, Young's modulus, and bending strength, were evaluated using a Universal Testing Machine (UTM) and three-point bending tests, while thermal conductivity was measured using a heat flow method. Physical properties such as surface

 doi:10.20944/preprints202602.1693.v1

appearance, bulk density, and water absorption were examined using optical microscopy (OM) and quantitative analysis. All results are reported in this study.

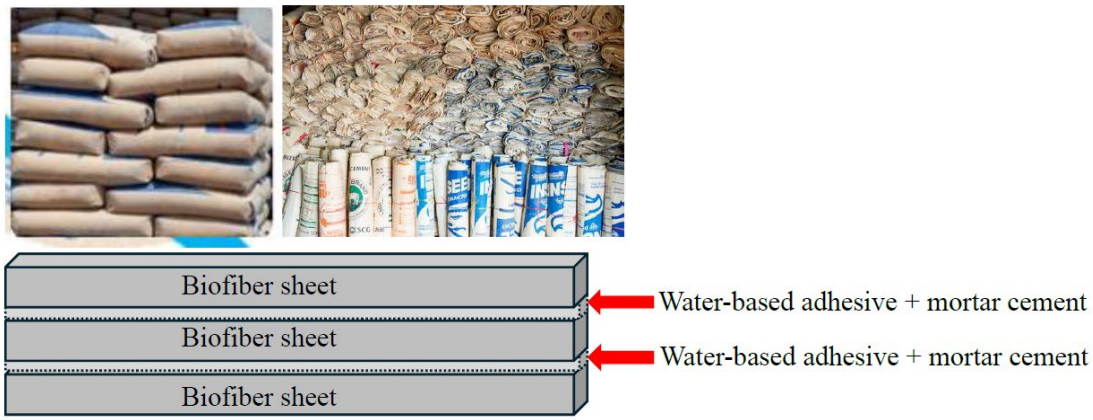

Scheme 5. Model of sample preparation.

2. Experimental

2.1. Materials

The primary raw materials consisted of 800 sheets of biofibers prepared from locally sourced cement packaging, each cut to dimensions of 7 × 30 cm. A water-based, starch-cellulosic adhesive was supplied by Nan Mee Co., Ltd. (Bangkok, Thailand). The water-based PVAc adhesive, composed of 90–95% deionized water and 6–11% polyvinyl acetate (PVAc, $[-CH_2-CH(OCOCH_3)-]_n$), is clear and colorless, with a pH of 5–8 and a specific gravity of 1.00–1.06. Portland cement was procured from Jorakay Co., Ltd. (Bangkok, Thailand). Its specifications are as follows: residue on 325-mesh screen ≈ 24%, maximum autoclave expansion 1%, minimum initial setting time 90 min, standard compressive strength 9 lb/in² at 7 days and 14.5 lb/in² at 28 days, air content in mortar 8–19% vol, and minimum water retention value 70%.

2.2. Instruments

A paper cutter (model: V-Virgin TS 125/115), with a power rating of 540 W and a maximum rotational speed of 12,000 rpm, was used to cut the cement packaging sheets.

Non-destructive testing (NDT) was conducted to inspect and evaluate the prepared samples using Visual Testing (VT). Visual observation, the first assessment method applied, was used to detect cracks, shrinkage, surface quality, and application feasibility in accordance with TISI 878-2023 and BS 874 standards.

The bulk density of the raw materials was calculated using $D = \frac{M}{V}$, where D is the bulk density (g/cm³), $M$is the sample mass (g), and $V$is the sample volume (cm³), derived from dimensional measurements.

An optical microscope (OM) (model: Olympus B51M) was employed to characterize the composite microstructures of the biofiber cement boards. The microscope uses visible light and optical lenses to generate magnified images. A 10× eyepiece was used to inspect surface defects such as cracks, shrinkage, and warping.

A Universal Testing Machine (UTM) (model: Hounsfield H50KS) was used to determine the mechanical properties of the biofiber cement boards, including tensile strength, stress, strain, and Young's modulus. The testing parameters were load of 500 N, strain range of 25%, crosshead speed of 50 mm/min, and preload of 1 N. A three-point bending test was also conducted using the UTM to evaluate flexural modulus, flexural stress, and flexural strain.

For a rectangular cross section:

 doi:10.20944/preprints202602.1693.v1

$$\sigma_f = \frac{3FL}{2bd^2} \tag{3}$$

For a circular cross section:

$$\sigma_f = \frac{FL}{\pi R^3} \tag{4}$$

Calculation of the flexural strain (ϵ_f):

$$\epsilon_f = \frac{6Dd}{L^2} \tag{5}$$

Calculation of flexural modulus (E_f):

$$E_f = \frac{L^3 m}{4bd^3} \tag{6}$$

where σ_f, ϵ_f, E_f, F, L, b, d, D, m, R according to σ_f = Modulus of Rupture (MPa); ϵ_f = Strain on the outer surface, (mm/mm); E_f = Flexural modulus of elasticity (MPa); F = load at a specific point on the load-deflection curve (N); L = Support span (mm); b = Width of test beam (mm); d = Depth/thickness of test beam (mm); D = Maximum deflection at beam center (mm); m = Initial slope of the load-deflection curve (N/mm); and R = Radius of specimen (mm).

ϵf A heat flow meter (model: EKO HC-074-200) was used to measure thermal conductivity in accordance with ASTM C518, ISO 8301, and JIS A1412. Tests were conducted between 20 °C and 50 °C, with the top plate maintained at a lower temperature than the bottom plate. Thermal conductivity was calculated based on Fourier's law using the measured heat flow through the specimen.

Water absorption and its effects on swelling or shrinkage were evaluated at room temperature (27 °C) according to ASTM D570 and ASTM D5890-11. Water absorption was calculated using:

$$Water\ Absorbtion\ (\%) = \frac{(W_2 - W_1)}{W_1}\ x\ 100 \tag{7}$$

where W_1 is the initial dry weight and W_2 is the weight after 24 h immersion.

Specimens were cut using a silicon carbide saw or equivalent equipment. Rectangular samples with parallel sides perpendicular to the forming surface were prepared, with a minimum volume of 25 cm^3. Loose particles were removed using compressed air. Mass was recorded to an accuracy of ±0.05 g using a weighing scale with ±0.01% precision. Samples were immersed in water at (20 ± 2)°C for at least 24 h. Successive mass readings at 2 h intervals were taken until variation was below 0.5%. After immersion, surface moisture was wiped off, and the saturated mass was recorded. Specimens were then oven-dried at (105 ± 5)°C using a forced-circulation oven until consecutive mass readings at 2 h intervals showed a decrease below 0.5%. Samples were cooled in a desiccator to ambient temperature, and dry mass was recorded.

2.3. Preparation of Multilayer Structural Composite Prototypes of Biofiber Cement Boards

The characteristics of the raw materials used to produce the biofiber cement boards are presented in Table 1. Prototype samples of biofiber cement blocks, illustrated in Scheme 5, were fabricated using cement packaging sheets, a water-based adhesive, and Portland cement. These prototypes were produced through casting and pressing based on the formulations listed in Table 2. The ratios of water, Portland cement, and water-based adhesive were 1:1:0, 1:1:1, and 1:1:2, respectively, combined with 72, 84, and 96 cement packaging sheets arranged in a stacked configuration, referred to as laminated structural composite materials. A total of nine formulations were developed and designated as Formula (x–y–z), where *x* denotes the number of biofiber cement

 doi:10.20944/preprints202602.1693.v1

packaging sheets, *y* represents the percentage of cement by volume, and *z* represents the percentage of water-based adhesive by volume. The prototype samples were prepared in bar and block shapes with uniform dimensions of 7.0 cm in width and 30.0 cm in length. The thickness of each specimen depended on the number of biofiber packaging sheets used in the respective formulation. Physical properties, including appearance, bulk density, water absorption, and dimensions—were assessed using non-destructive testing (NDT). Visual inspection was performed to evaluate appearance, dimensions were measured using a vernier caliper, and water absorption was determined through immersion testing. Mechanical properties were evaluated using a universal testing machine (UTM) with a three-point bending configuration, and the results are summarized in Table 3.

Table 1. Characteristics of Raw Materials for Biofiber Cement Board Production.

Characteristics	Biofiber sheets	Water-based PVAc adhesive	Portland cement
Weight (g/m²)	40-50	-	-
Thickness (mm)	60-80	-	-
Bulk density (g/cm³)	1.55-1.60	1.0-1.60	3.14-3.20
True density (g/cm³)	0.61-0.65	1.0	2.07
Moisture (%)	7.5-9.0	58	-
Ash content (%)	0-12	3.0-4.5	0.52-1.00
Brightness (ISO), (%)	62-65	-	-
Opacifier (%)	90-94	48	> 96
Tensile strength (MPa)	45-60	> 17	1.70
Compressive strength 2 days (MPa)	-	10-15	26.60
Compressive strength 7 days (MPa)	-	-	40.80
Compressive strength 28 days (MPa)	-	-	55.80
Color	83.7 L*, -0.450 a*, 5.10 b*	Colorless, odorless liquid	Gray-color, fine solid powder
Consistency (%)	-	High viscosity (20-80 poise)	17-30
Solubility	Insoluble in water	Water soluble	Standard water requirement 27%
pH	7.45 - 7.79	5-8	12.50-13.50
Water content (%)	-	90-95	-
Polyvinyl acetate (%)	-	6-11	-

Remark: " – " indicates not measured. L^* means perceptual light, while a^* and b^* represent the four unique colors perceived by human vision: red, green, blue, and yellow.

Table 2. Sample Preparation (Mean ± Standard Deviation, n = 5).

Sample	Ratio (Water: Portland Cement: Water-Based PVAc Adhesive) (%Vol.)	Biofiber cement packaging (layers)	Portland Cement (% Vol.)	Water-Based PVAc Adhesive (ml)	Water (ml)
Formula 1 (72-200-0)	1:1:0	72	200	0	200
Formula 2 (84-200-0)	1:1:0	84	200	0	200
Formula 3	1:1:0	96	200	0	200

 doi:10.20944/preprints202602.1693.v1

(96-200-0)					
Formula 4 (72-200-200)	1:1:1	72	200	200	200
Formula 5 (84-200-200)	1:1:1	84	200	200	200
Formula 6 (96-200-200)	1:1:1	96	200	200	200
Formula 7 (72-200-400)	1:1:2	72	200	400	200
Formula 8 (84-200-400)	1:1:2	84	200	400	200
Formula 9 (96-200-400)	1:1:2	96	200	400	200

Remark: Density of cement is 1.44 g/cm^3 (ϱ=1.44 g/cm^3). Formulas 1, 2, and 3 were used as reference samples. In Formula (x-y-z); *x* represents the number of biofiber sheets, *y* is the percentage of cement by volume, and *z* represents the percentage of water-based PVAc adhesive by volume.

Table 3. Characterization of Biofiber Cement Boards.

Characterization	Measurement	Standard method	Testing
Physical Properties	Appearance Dimension Thickness Bulk density Swelling	ASTM D570 and ASTM D5890-11	Nondestructive testing (NDT) Vernier Caliper Calculation
Mechanical Properties	Bending Strength Tensile Strength Tensile Young's Modulus Compressive Strength		UTM and 3-Point Bending Tests
Thermal Properties	Thermal conductivity	ASTM C518, ISO-8301, and JIS-A1412	heat flow meter (EKO), (HC-074-200)

The combination of cement and biofiber sheets accelerates curing through an exothermic thermochemical reaction. Curing involves retaining sufficient moisture in the cement within an appropriate temperature range to promote hydration during the early stages. Hydration is the chemical reaction between water and cement that produces compounds responsible for the setting and hardening of the material. During curing, the heat released by the exothermic reaction also accelerates the curing of the water-based adhesive, thereby enhancing the strength and toughness of the biofiber cement boards. Formulations with higher adhesive content demonstrated improved bonding strength due to increased ionic chemical bonds and covalent interactions between the adhesive and cement layers compared to those containing little or no adhesive.

3. Results and Discussion

3.1. Characteristics and Physical Properties of Biofiber Cement Boards

The physical properties of the biofiber cement boards—including appearance, dimensions, thickness, bulk density, and water absorption percentage—were evaluated using the standard methods listed in Table 5, and the results are presented in Table 4. Visual observations are shown in Figures 1–3. The ratio of Portland cement to water-based adhesive significantly affected the appearance, dimensions, and thickness of both the longitudinal and transverse sections of the samples. Among all samples, Formulas 7, 8, and 9 demonstrated the most desirable appearance and

 doi:10.20944/preprints202602.1693.v1

physical properties (in terms of bulk density and water absorption), with no signs of warping or shrinkage. As the number of cement packaging sheets increased, the bulk density also increased. However, when the number of cement packaging sheets was held constant, increasing the ratio of Portland cement to water-based PVAc adhesive resulted in a decrease in bulk density, as shown in Table 4 and Figure 3a. This behavior occurs because the water content in the PVAc adhesive participates in cement hydration, while the hydroxyl groups in PVAc chemically and physically interact with hydration products such as C–S–H and Ca $(OH)_2$. Additionally, PVAc chains form a polymer–cement composite network, which lowers bulk density while simultaneously enhancing chemical bonding, mechanical strength, and durability. Formulas 7, 8, and 9 exhibited the lowest bulk densities, measured at 1.034 ± 0.108, 1.090 ± 0.120, and 1.300 ± 0.135 g/cm^3, respectively. These values fall within the standard bulk density range for building materials, as illustrated in Scheme 2. All observed physical characteristics and performance values comply with industrial standards TISI 878:2023 and BS 874, as summarized in Table 5 and Table 6. Water absorption percentage also decreased progressively, with Formulas 7, 8, and 9 showing particularly low values of 0.1239 ± 0.0202%, 0.1044 ± 0.0200%, and 0.0835 ± 0.0102%, respectively. These formulations displayed smooth surfaces with no visible warping or shrinkage.

These formulations displayed smooth surfaces with no visible warping or shrinkage.

Table 4. Physical Properties of Biofiber Cement Boards.

Sample	Ratio of Portland cement to water-based adhesive	Thickness (cm) (avg ± S.D.)	Length (cm) (avg ± S.D.)	Width (cm) (avg ± S.D.)	Bulk Density (g/cm^3) (avg ± S.D.)
Formula 1 (72-200-0)	1:0	1.06 ± 0.29	22.00 ± 4.93	7.00 ± 0.00	1.109 ± 0.185
Formula 2 (84-200-0)	1:0	1.51 ± 0.20	30.00 ± 2.03	7.00 ± 0.01	1.191 ± 0.127
Formula 3 (96-200-0)	1:0	1.60 ± 0.15	31.00 ± 3.80	7.00 ± 0.10	1.316 ± 0.120
Formula 4 (72-200-200)	1:1	1.01 ± 0.23	21.00 ± 4.00	7.00 ± 0.01	1.049 ± 0.134
Formula 5 (84-200-200)	1:1	1.22 ± 0.15	25.00 ± 3.89	7.00 ± 0.03	1.113 ± 0.160
Formula 6 (96-200-200)	1:1	1.47 ± 0.21	29.00 ± 4.20	7.00 ± 0.20	1.312 ± 0.158
Formula 7 (72-200-400)	1:2	0.58 ± 0.34	14.50 ± 5.40	7.00 ± 0.20	1.034 ± 0.108
Formula 8 (84-200-400)	1:2	1.11 ± 0.29	23.00 ± 4.80	7.00 ± 0.03	1.090 ± 0.120
Formula 9 (96-200-400)	1:2	1.21 ± 0.24	24.50 ± 4.35	7.00 ± 0.04	1.300 ± 0.135

Remark: Density of cement is 1.44 g/cm^3 (ρ=1.44 g/cm^3). Formulas 1, 2, and 3 were acted as reference samples. Formula (x-y-z); *x* represents the number of biofiber sheets, *y* is the percentage of cement by volume (% vol.), and *z* is the percentage of water-based PVAc adhesive by volume (% vol).

 doi:10.20944/preprints202602.1693.v1

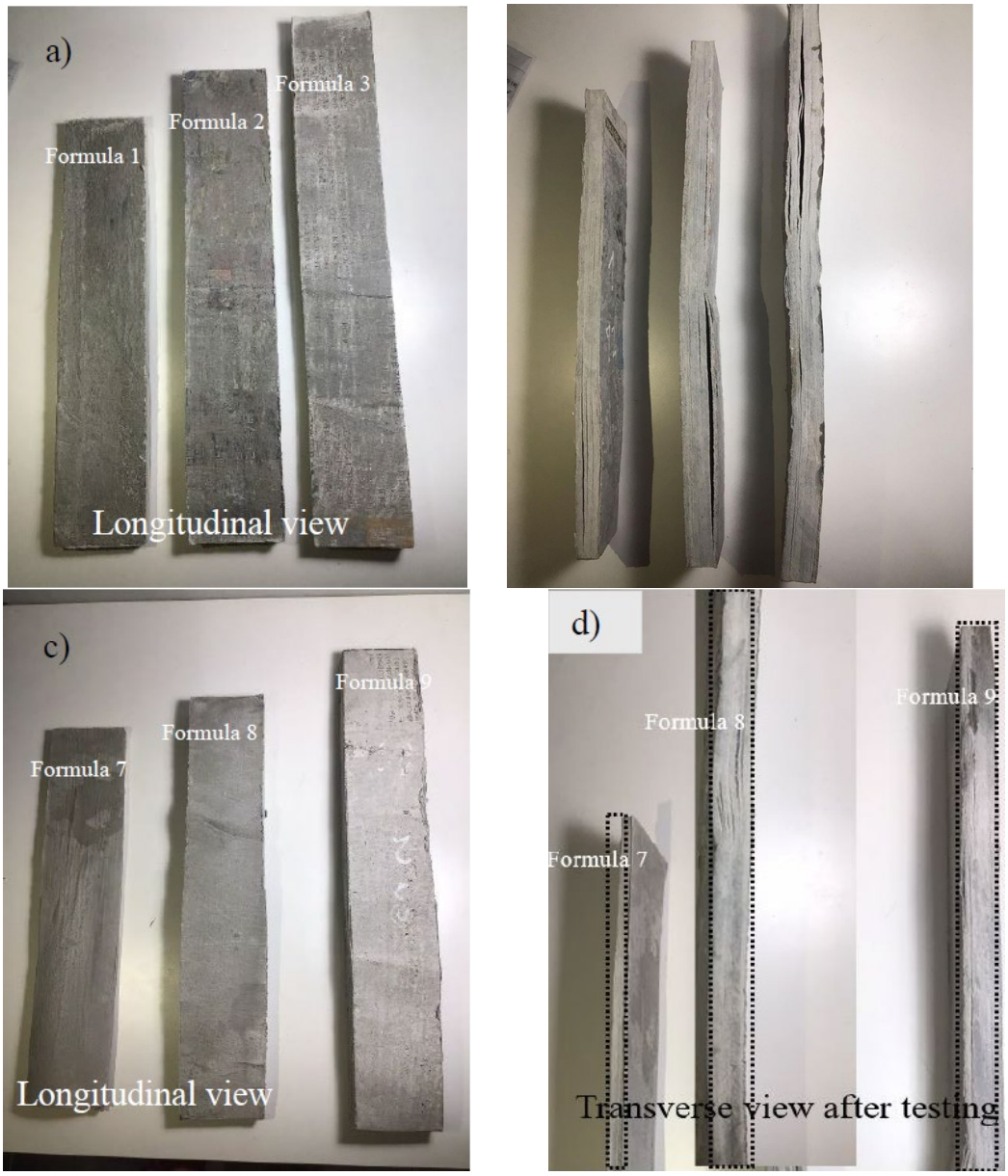

Figure 1. Biofiber cement boards after UTM testing: (a) Longitudinal sections of samples (Formulas 1, 2, and 3); (b) Transverse sections of samples (Formulas 4, 5, and 6); (c) Longitudinal sections of samples (Formulas 7, 8, and 9); (d) Transverse sections of samples (Formulas 7, 8, and 9).

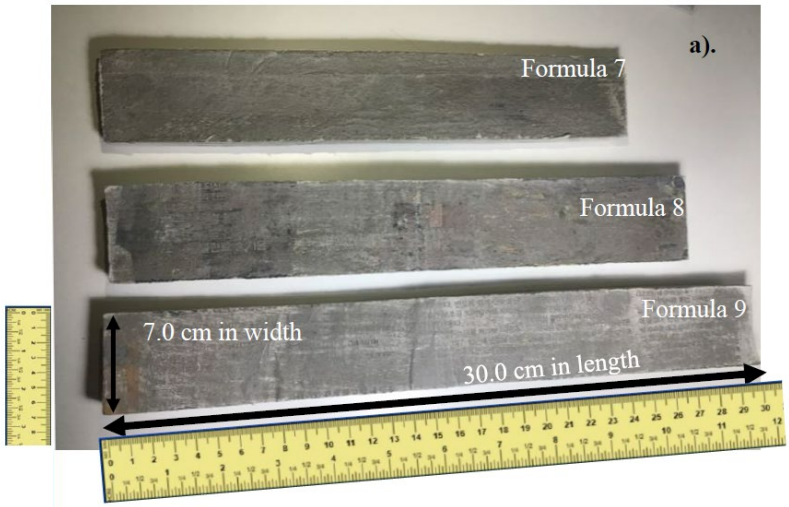

 doi:10.20944/preprints202602.1693.v1

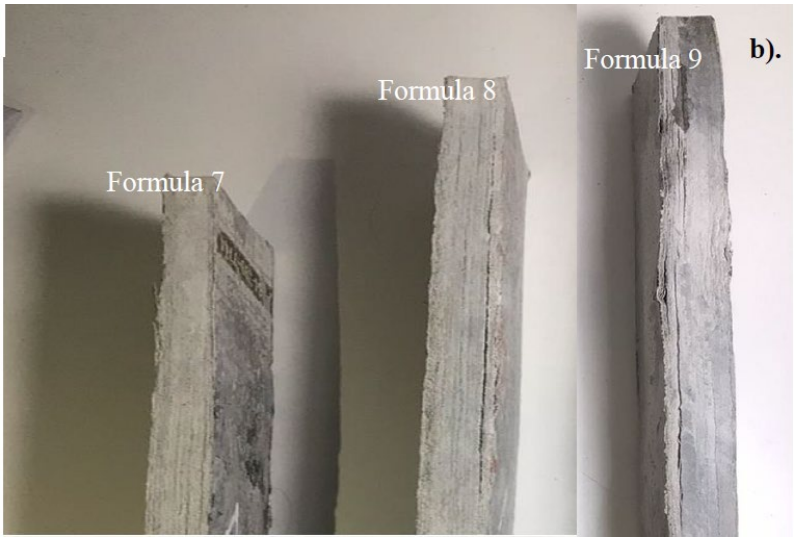

Figure 2. Dimensions and optimal biofiber cement boards after UTM testing: (a) Longitudinal sections of samples (Formulas 7, 8, and 9) and (b) Transverse sections of samples (Formulas 7, 8, and 9).

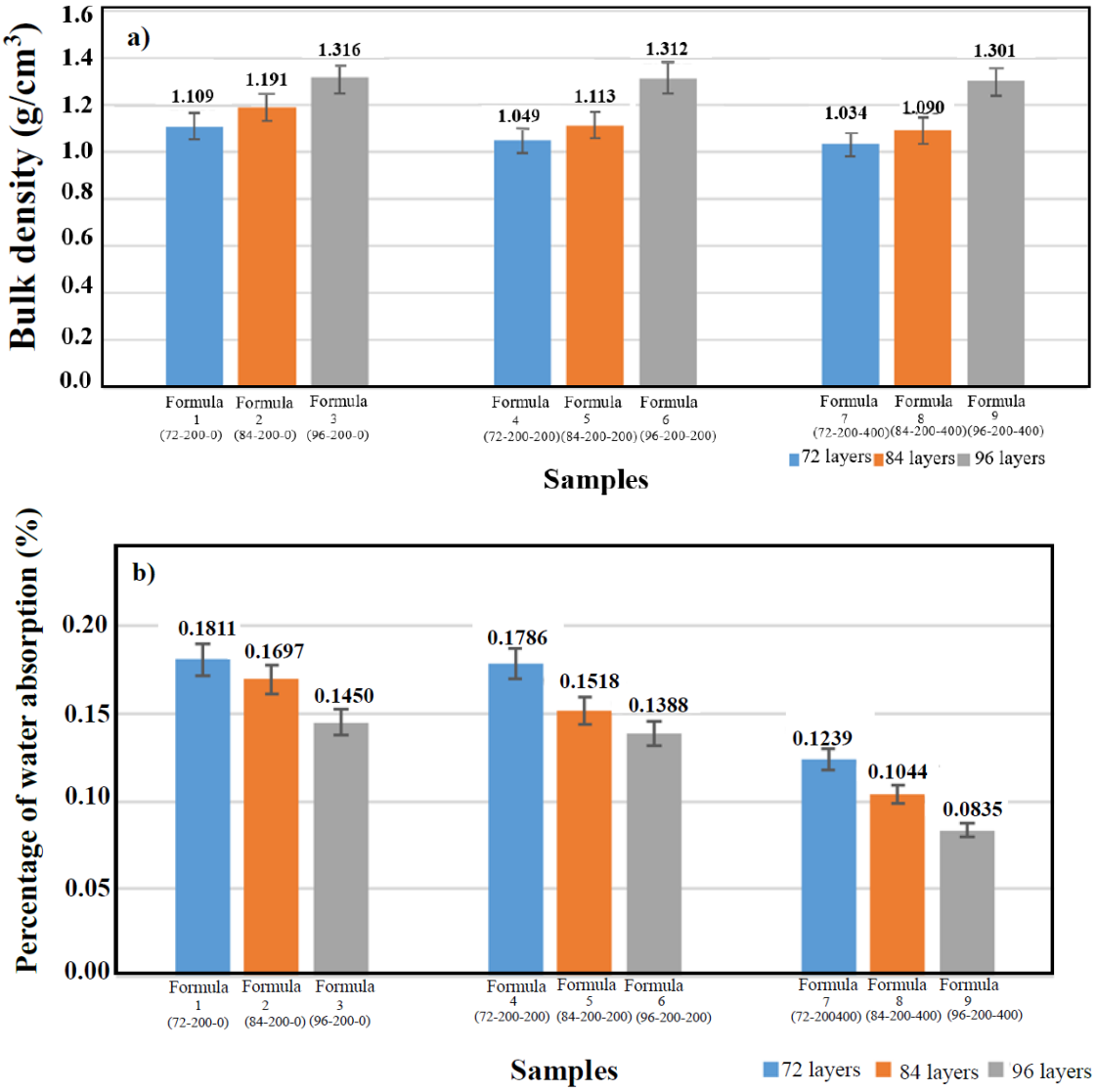

Figure 3. Physical properties of biofiber cement boards: (a) Bulk density and (b) Water absorption percentage.

 doi:10.20944/preprints202602.1693.v1

All observed physical characteristics and performance values comply with industrial standards TISI 878:2023 and BS 874, as summarized in Table 5.

Table 5. Industrial Standard TISI no. 878:2023 and BS 874.

No.	Determined Standards	Standard Values
1.	Bulk Density	1.100 - 1.300 kg/m^3
2.	Humidity	9.00 - 15.00%
3.	Thermal Conductivity	Less than 0.155 W/m. K
4.	Swelling upon Immersion in Water	Less than 2.00%
5.	Flexural Strength or Bending Strength	Not less than 9 MPa
6.	Young's Modulus of Elasticity	Not less than 3000 MPa
7.	Tensile Stress	Not less than 0.5 MPa

Remark: TISI stands for the Thai Industrial Standards Institute, as specified in TISI 878:2023 for Cement-Bonded Particleboards: High Density. BS 874 refers to the British Standard for methods of determining thermal insulating properties.

Table 6. Physical Properties and Water Absorption of Biofiber Cement Boards.

Sample	Ratio of cement and water glue	Water absorption percentage (%)	Physical properties (Appearance)
Formula 1 (72-200-0)	1:0	0.1811 ± 0.0185	Good appearance in the longitudinal area but swollen and warped in the cross-sectional area.
Formula 2 (84-200-0)	1:0	0.1697 ± 0.0180	Good appearance in the longitudinal area, but the cross-sectional area is prone to swelling and warping.
Formula 3 (96-200-0)	1:0	0.1450 ± 0.0093	Good appearance in the longitudinal area, but the cross-sectional area is prone to easy swelling and warping.
Formula 4 (72-200-200)	1:1	0.1786 ± 0.0203	Good appearance in the longitudinal area, but the cross-sectional area is slightly swollen and warped.
Formula 5 (84-200-200)	1:1	0.1518 ± 0.0200	Good appearance in the longitudinal area, but the cross-sectional area is slightly swollen and warping.
Formula 6 (96-200-200)	1:1	0.1388 ± 0.0104	Good appearance in the longitudinal area, but the cross-sectional area is slightly swollen and warped.
Formula 7 (72-200-400)	1:2	0.1239 ± 0.0202	Both longitudinally and tranversly, the appearance was good: smooth plate, with no warping or shrinkage.
Formula 8 (84-200-400)	1:2	0.1044 ± 0.0200	Both longitudinally and tranversly, the appearance was good, with a smooth plate, no warping, and no shrinkage.
Formula 9 (96-200-400)	1:2	0.0835 ± 0.0102	Both longitudinally and tranversly, the appearance was good, with a smooth plate, no warping, and no shrinkage.

Remark: Density of cement is 1.44 g/cm^3 (ϱ=1.44 g/cm^3). Formulas 1, 2, and 3 were acted as reference samples. Formula (x-y-z); x represents the number of biofiber sheets, y is the percentage of cement by volume (% vol.), and z is the percentage of water-based PVAc adhesive by volume (% vol).

 doi:10.20944/preprints202602.1693.v1

3.2. Mechanical and Thermal Properties of Biofiber Cement Boards

The mechanical properties, including bending strength, Young's modulus, and tensile strength, were measured and are summarized in Table 7 and Figures 4 and 5. The results show a consistent upward trend across all three properties. As the ratio of Portland cement to water-based adhesive increased from 1:0 to 1:1 to 1:2, tensile strength, bending strength, and Young's modulus also increased proportionally. Additionally, increasing the number of biofiber cement packaging sheets further contributed to the improvement of these properties, as shown in Table 7. Among all compositions, Formulas 7, 8, and 9 exhibited the highest performance, with tensile strengths of 15.085 ± 0.560, 17.890 ± 0.350, and 19.489 ± 0.670 MPa, bending strengths of 15.650 ± 2.609, 18.258 ± 2.555, and 20.867 ± 2.505 MPa, and moduli of elasticity of 4301.500 ± 185.650, 5018.000 ± 211.230, and 5735.068 ± 387.032 MPa, respectively (Figure 5). These results indicate that incorporating cement together with a small proportion of water-based PVAc adhesive into laminated recycled cement packaging sheets produces composites with high compressive strength suitable for industrial and construction applications.

Table 7. Mechanical Properties of Biofiber Cement Boards.

Sample	Tensile strength (MPa)	Tensile Strain (%)	Bending Strength (MPa)	Young's modulus of Elasticity (MPa)	Thermal Conductivity (W/m.K)
Formula 1 (72-200-0)	3.485 ± 0.245	> 10	3.528 ± 0.588	281.500 ± 25.310	N/A
Formula 2 (84-200-0)	4.180 ± 0.165	> 10	4.116 ± 0.0500	328.417 ± 15.890	N/A
Formula 3 (96-200-0)	4.756 ± 0.152	> 10	4.704 ± 0.350	384.000 ± 51.311	N/A
Formula 4 (72-200-200)	6.350 ± 0.285	> 10	6.340 ± 1.007	1401.000 ± 100.501	N/A
Formula 5 (84-200-200)	6.950 ± 0.115	> 10	7.397 ± 1.058	1635.000 ± 233.501	N/A
Formula 6 (96-200-200)	8.056 ± 0.220	> 10	8.453 ± 1.057	1868.500 ± 150.650	N/A
Formula 7 (72-200-400)	15.085 ± 0.560	> 10	15.650 ± 2.609	4301.500 ± 185.650	0.149
Formula 8 (84-200-400)	17.890 ± 0.350	> 10	18.258 ± 2.555	5018.000 ± 211.230	0.150
Formula 9 (96-200-400)	19.489 ± 0.670	> 10	20.867 ± 2.505	5735.068 ± 387.032	0.152

Remark: Tensile strength of reference Portland cement: 1.7 MPa, Compressive strength of reference Portland cement: 47.21 MPa, Flexural strength of reference Portland cement: 6.51 MPa, Thermal conductivity of reference Portland cement (dry state): 1.79 W/m.K, Bulk density of reference mortar cement: 2.07 g/cm^3.

 doi:10.20944/preprints202602.1693.v1

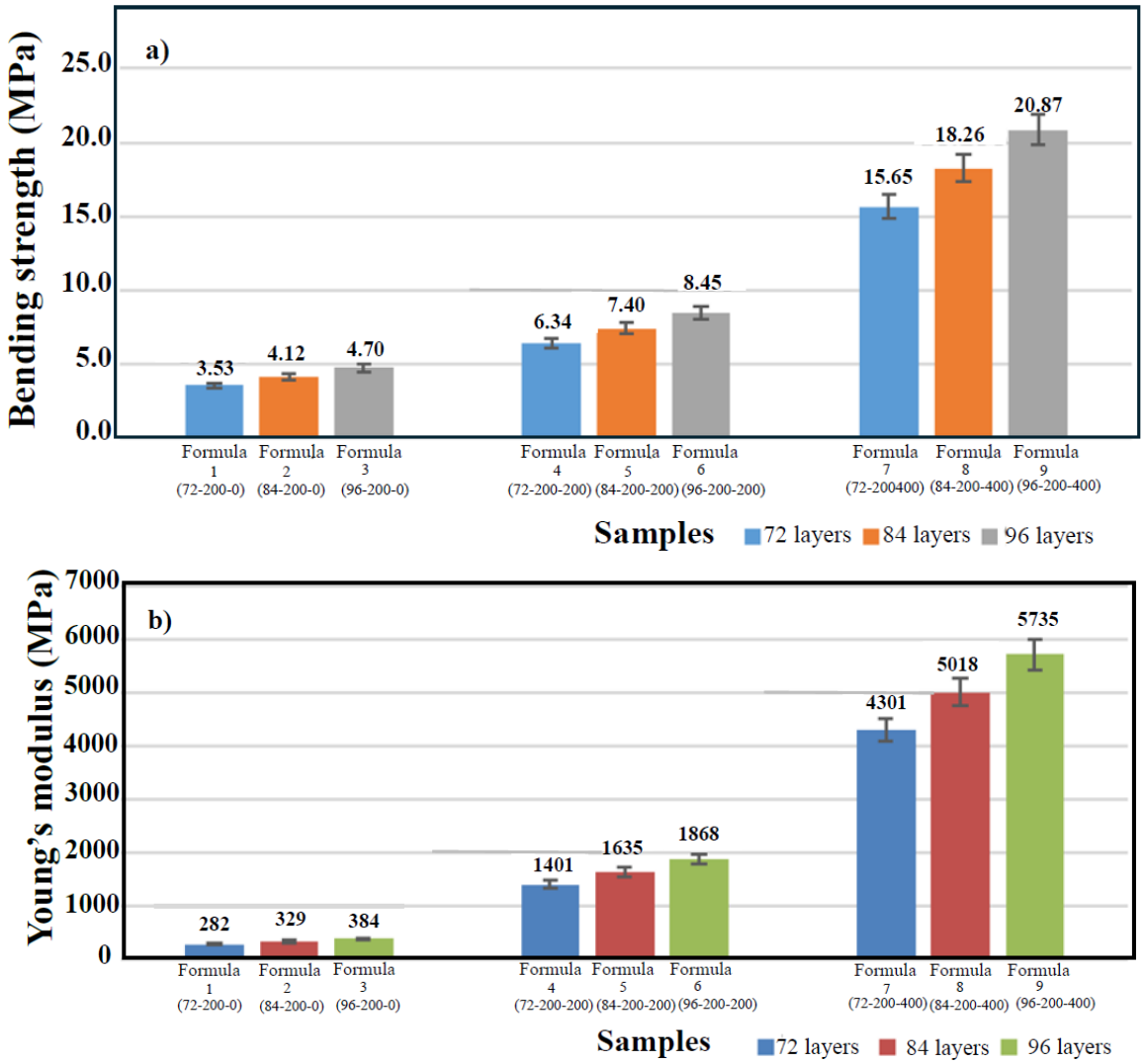

Figure 4. Mechanical properties of biofiber cement boards: (a) Bending strength and (b) Young's modulus.

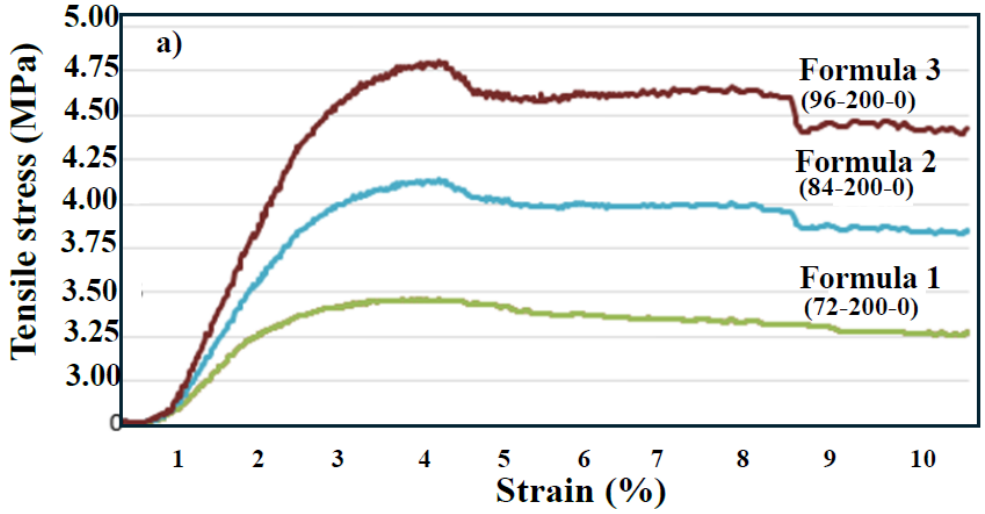

 doi:10.20944/preprints202602.1693.v1

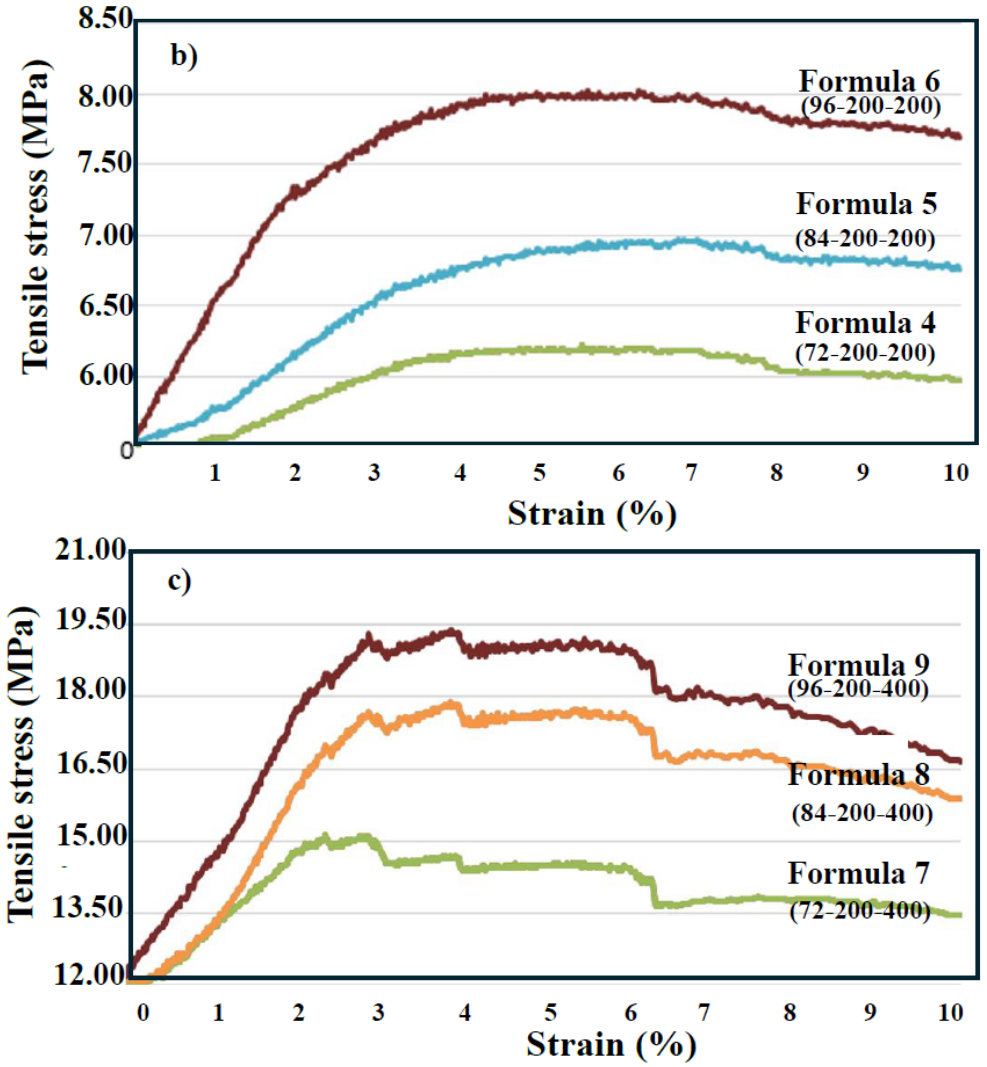

Figure 5. Relationship between tensile stress and strain of biofiber cement boards: (a) Formulas 1, 2, and 3; (b) Formulas 4, 5, and 6; and (c) Formulas 7, 8, and 9.

During cement hydration, water reacts with cement in an exothermic process that leads to hardening. The addition of PVAc improves workability and adhesion by interacting with cement while simultaneously adhering to the recycled cement packaging fibers. During curing, the PVAc polymer forms a film that bonds with the cement matrix, reinforcing the microstructure and enhancing internal cohesion. As a result, the mechanical performance of the biofiber cement boards is significantly improved. These findings are consistent with previous studies: Wong et al. reported improved mechanical strength after incorporating burnt newspaper ash particles into cement [37]; Rajput et al. produced building materials from recycled paper mill waste with 10 wt% Portland cement [38]; Sales et al. demonstrated that fiberboard panels from reclaimed paper bags improved both flexural strength and elastic modulus [39]; and Ardanuy et al. confirmed that cellulose fiber reinforcement enhances the mechanical, physical, and durability properties of cement composites [40].

Thermal properties were evaluated using a heat flow meter for samples corresponding to Formulas 7, 8, and 9, as listed in Table 7. The thermal conductivity values were 0.149, 0.150, and 0.152 W/m·K, respectively, which fall within the acceptable range for cement-bonded particleboards specified in TISI 878:2023 and BS 874 standards (<0.155 W/m·K; Table 5). The recycled biofiber sheets act as cellulose-based reinforcement that introduce air-filled pores, which reduce thermal conductivity due to the insulating nature of air. The PVAc film stabilizes these pores, preventing collapse during curing and resulting in a lightweight structure with enhanced thermal insulation. Typically, cement alone has a relatively high thermal conductivity (~1.01 W/m·K), whereas PVAc

 doi:10.20944/preprints202602.1693.v1

has a much lower value (~0.18 W/m·K). Therefore, incorporating PVAc into the cement matrix decreases the effective thermal conductivity, improving resistance to heat transfer. Furthermore, while cement hydration releases heat, PVAc partially coats cement grains, slowing hydration and moderating heat release, thus reducing the risk of thermal cracking. In addition, PVAc forms bonds with Ca^{2+} ions and hydrogen bonds with cellulose fibers from the biofiber cement sheets, creating a polymer–fiber–cement network that retains moisture and buffers temperature fluctuations. Although PVAc is organic, it becomes encapsulated within the cement matrix. Cement is inherently fire-resistant, and the PVAc–cellulose network promotes char formation, which acts as a thermal barrier, slowing heat penetration and improving fire resistance. A comparison of the mechanical, thermal, and physical properties of the biofiber cement boards with relevant standard requirements—including bulk density, bending strength, Young's modulus, tensile strength, water absorption, and thermal conductivity—is presented in Table 8. Formulas 7, 8, and 9 demonstrated the most favorable overall performance, meeting the standard criteria for biofiber cement boards and related building materials.

Table 8. Comparison of Obtained Results with Standard Values.

Qualification test	Formula 1 (72-200-0)	Formula 2 (84-200-0)	Formula 3 (96-200-0)	Formula 4 (72-200-200)	Formula 5 (84-200-200)	Formula 6 (96-200-200)	Formula 7 (72-200-400)	Formula 8 (84-200-400)	Formula 9 (96-200-400)
Bulk density	√	√	√	√	√	√	√	√	√
Bending strength	x	x	x	x	x	x	√	√	√
Young's modulus	x	x	x	x	x	x	√	√	√
Tensile strength	x	x	x	x	x	x	√	√	√
Swelling in water	√	√	√	√	√	√	√	√	√
Thermal conductivity	-	-	-	-	-	-	√	√	√
Other physical properties and characteristics	x	x	x	x	x	x	√	√	√

Remark: Bulk Density: √ indicates that the value falls within the standard range of 1.100 - 1.300 kg/m³. Bending strength: Measured using the three-point bending method. A "-" under thermal conductivity indicates that the value was not measured.

4. Conclusion

Biofiber cement boards were successfully fabricated as structural composite materials. The cement packaging biofiber sheets functioned as the reinforcing phase, while Portland cement and water-based PVAc adhesive served as the matrix phase. Increasing the number of biofiber sheets led to improvements in the physical, mechanical, and thermal properties of the boards. Additionally, higher ratios of Portland cement to water-based adhesive further enhanced these properties. The most suitable formulations identified in this study were Formulas 7, 8, and 9, which exhibited the following performance ranges:

- **Tensile Strength:** 15.085 ± 0.560, 17.890 ± 0.350, and 19.489 ± 0.670 MPa, respectively
- **Bending Strength:** 15.650 ± 2.609, 18.258 ± 2.555, and 20.867 ± 2.505 MPa, respectively
- **Modulus of Elasticity:** 4301.500 ± 185.650, 5018.000 ± 211.230, and 5735.068 ± 387.032 MPa, respectively

All physical, mechanical, and thermal properties measured were consistent with and fell within the standard limits specified by ASTM D570, ASTM D5890-11, ASTM C518, ISO 8301, and JIS A1412. The thermal conductivity values of Formulas 7, 8, and 9—0.149, 0.150, and 0.152 W/m·K, respectively—also meet the criteria for insulation materials suitable for decorative applications, ceiling panels, and wall construction. Furthermore, tweremechanical strength of the biofiber cement

 doi:10.20944/preprints202602.1693.v1

board samples were approximately 5–10 times higher than that of the reference formulation with the lowest Portland cement-to-water-based adhesive ratio (1:0).

Supplementary Materials: The following supporting information can be downloaded at the website of this paper posted on Preprints.org.

Author Contributions: Conceptualization, Nuchnapa Tangboriboon; Methodology, Panisara Panthongkaew; Formal analysis, Panisara Panthongkaew; Investigation, Panisara Panthongkaew; Resources, Panisara Panthongkaew; Data curation, Nuchnapa Tangboriboon; Writing – original draft, Nuchnapa Tangboriboon; Visualization, Nuchnapa Tangboriboon; Supervision, Nuchnapa Tangboriboon; Project administration, Nuchnapa Tangboriboon.

Data Availability Statement: The original contributions presented in this study are included in the article/supplementary material. Further inquiries can be directed to the corresponding author.

Acknowledgments: The authors extend their sincere gratitude to the Department of Materials Engineering, Kasetsart University, Bangkok, Thailand, for granting access to the analytical equipment essential for this research.

Conflicts of Interest: The authors declare that there are no conflicts of interest.

References

1. Wong, L.S., Chandran, S.N., Rajasekar, R.R., Kong, S.Y. Pozzolanic characterization of waste newspaper ash as a supplementary cementing material of concrete cylinders. *Case Stud. Constr. Mater.* 2022 (17), e01342.
2. Xia, G., Wan, J., Zhang, J., Zhang, X., Xu, L., Wu, J., He, J., Zhang, J. Cellulose-based films prepared directly from waste newspapers via anionic liquid, *Carbohydr. Polym.* 2016 (151), 223–229.
3. Okada, K., Yamamoto, N., Kameshima, Y., Yasumori, A. Porous properties of activated carbons from waste newspaper prepared by chemical and physical activation. *J. Colloid Interface Sci.* 2003 (262/1), 179-193.
4. Das, S. Mechanical and water swelling properties of wastepaper reinforced unsaturated polyester composites. *Constr. Build. Mater*. 2017 (138), 469-478.
5. Zhou, Z., Liu, T., Tan, Y., Zhou, W., Wang, Y., Shi, S.Q., Gong, S., Li, J. A high-performance, full-degradable bioinspired newspaper-based composite enhanced by borate ester bonds. *Compos. Sci. Technol. 2023 (241), 110130.*
6. Lim, M., Kwon, H., Kim, J., Seo, J., Han, H. Khan, S.B. Highly-enhanced water resistant and oxygen barrier properties of cross-linked poly(vinyl alcohol) hybrid films for packaging applications. *Prog. Org. Coat.* 2015 (85), 68-75.
7. Agyeman, S., Obeng-Ahenkora, N.K., Assiamah, S., Twumasi, G. Exploiting recycled plastic waste as an alternative binder for paving blocks production. *Case Stud. Constr. Mater.* 2019 (11), e00246.
8. Kunaver, M., Medved, S., Čuk, N., Jasiukaityté, E., Poljanšek, I., Strnad, T. Application of liquefied wood as a new particle board adhesive system. *Bioresour. Technol.* 2010 (101/4), 1361-1368.
9. Mazaherifar, M.H., Coșereanu, C., Timar, C. M., Georgescu, S.V. Physical and mechanical properties of foam-type panels manufactured from recycled cardboard. *Constr. Build. Mater*. 2024 (411). 134685.
10. Jensen, M. S., Alfieri, P.V. Design and manufacture of insulation panels based on recycled lignocellulosic waste. *Clean. Eng. Technol.* 2021 (3), 100111.
11. Bayatkashkoli, A., Ramazani, O., Keyani, S., Mansouri, H.R., Madahi, N.K. Investigation on the production possibilities of high-pressure laminate from borax and recycled papers as a cleaner product. *J. Clean. Prod*. 2018 (192), 775-781.
12. Ferreira, G., Das, S., Rego, A., Silva, R.R.A., Gaspar, D., Goswami, S., Pereira, R. N., Fortunato, E., Pereira, L., Martins, R., Nandy, S. Eco-designed recycled newspaper for energy harvesting and pressure sensor applications. *J. Chem. Eng*. 2024 (480), 147995.

13. Křížová, K., Baránek, S., Bubeník, J., Mazán, T. Study of the behaviour of recycled and traditional fibres in cement composite at extreme temperatures. *J. Build. Eng*. 2024 (95), 110134.
14. Chen, S., Chen, Y., Li, D., Xu, Y., Xu, F. Flexible and Sensitivity-Adjustable Pressure Sensors Based on Carbonized Bacterial Nanocellulose/Wood-Derived Cellulose Nanofibril Composite Aerogels. *ACS Appl. Mater. Interfaces*. 2021 (13/7), 8754-8763,
15. Basarir, F., Kaschuk, J.J., Vapaavuori, J. Perspective about Cellulose-Based Pressure and Strain Sensors for Human Motion Detection. *Biosens.* 2022 (12/4), 187.
16. Muddasar, M., Beaucamp, A., Culebras, M., Collins, M.N. Characteristics and applications for rechargeable batteries. *Int. J. Biol. Macromol*. 2022 (219), 788-803.
17. Yang, C. Wu, Q., Xie, W., Zhang, X., Brozena, A., Zheng, J., Garaga, M.N., Ko, B.H., et. al. Copper-coordinated cellulose ion conductors for solid-state batteries. *Nat.* 2021 (598), 590-596.
18. Goswami, S., Nandy, S., Calmeiro, T.R., Igreja, R., Martins, R., Fortunato, E. Stress Induced Mechano-electrical Writing-Reading of Polymer Film Powered by Contact Electrification Mechanism. *Sci. Rep*. 2016 (6), 1-10.
19. Wohlert, M., Benselfelt, T., Wågberg, L., Furó, I., Berglund, L.A., Wohlert, J. Cellulose and the role of hydrogen bonds: not in charge of everything. *Cellulose*. 2022 (29), 1-23.
20. Wu, J., Che, X., Hu, H.C., Xu, H., Li, B., Liu, Y., Li, J., Ni, Y., Zhang, X., Ouyang, X. Organic solar cells based on cellulose nanopaper from agroforestry residues with an efficiency of over 16% and effectively wide-angle light capturing. *J. Mater. Chem*. A. 2020 (8/11), 5442-5448.
21. Vicente, A.T., Araújo, A., Mendes, M.J., Nunes, D., Oliveira, M.J., et. al. Multifunctional cellulose-paper for light harvesting and smart sensing applications. *J. Mater. Chem. C*. 2018 (6), 3143-3181.
22. Cui, X., Huang, F., Zhang, X., Song, P., Zheng, H., Chevali, V., Wang, H., Xu, Z. Flexible pressure sensors via engineering microstructures for wearable human-machine interaction and Health Monitoring Applications. *iScience.* 2022 (25/4), 104148.
23. Tafete, G.A., Abera, M.K., Thothadri, G. Review on nanocellulose-based materials for supercapacitors applications. *J. Energy Storage*. 2022 (48), 103938.
24. Sun, Z., Qu, K., You, Y., Huang, Z., Liu, S., Li, J., Hu, Q., Guo, Z. Overview of cellulose-based flexible materials for supercapacitors. *J. Mater. Chem. A*. 2021 (9), 7278-7300.
25. Haršányová, T., Bauerová, K., Matušová, D. Matrix adhesive system containing plant extract. *Chemical Monthly. 2018 (149), 883-885.*
26. Oktay, S., Pizzi, A., Koken, N., Bengü, B. Chemical modification techniques of corn starch for synthesis wood adhesive. *Int. J. Adhes. Adhes.* 2024 (128), 103545.
27. Xu, Y., Zhang, Q., Lei, H., Zhou, X., Zhao, D., Du, G., Pizzi, A., Xi, X. A formaldehyde-free amino resin alternative to urea-formaldehyde adhesives: A bio-based oxidized glucose – urea resin. *Ind. Crop. Prod.* 2024 (218), 119037.
28. Li, J., Huan, X., Wang, S., Sheng, Y., Xu, D., You, Z. Performance of optimized composition of epoxy resin adhesive used in High Friction Surface Treatment. *Case Stud. Constr. Mater.* 2024 (21), e03431.
29. Lyu, Y., Zhan, Y., Li, J., Fang, G. A tough, strong, and fast-curing phenolic resin enabled by dopamine-grafted chitosan and polyethyleneimine-functionalized graphene. *Int. J. Biol. Macromol*. 2024 (279), 135472.
30. Dorieh, A., Ayrilmis, N., Pour, M.F., Movahed, S.G., Kiamahallen, M.V., et al. Phenol formaldehyde resin modified by cellulose and lignin nanomaterials: Review and recent progress. *Int. J. Biol. Macromol*. 2022 (222), 1888-1907.
31. Tsybril, Y., Nosko, O., Zglobicka, I., Kuciej, M. Emission and properties of airborne wear particles from train brake friction materials based on novolac phenolic resins and butadiene rubbers. *Wear.* 2024 (546-547), 205332.
32. Hazwan Hussin, M., Latif, N.H.A., Hamidon, T.S., Idris, N.N. et al. Latest advancements in high-performance bio-based wood adhesives: A critical review. *J. Mater. Res. Technol*. 2022 (21), 3909-3946.
33. Tian, X., Lv, S., Zhang, J., Yu, L., Liu, X., Xin, X. Recent advancement in synthesis and modification of water-based acrylic emulsion and their application in water-based ink: A comprehensive review. *Prog. Org. Coat*. 2024 (189), 108320.

 doi:10.20944/preprints202602.1693.v1

34. Ashori, A., Tabarsa, T., Valizadeh, I. Fiber reinforced cement boards made from recycled newsprint paper. *Mater. Sci. Eng. A*. 2011 (528), 7801-7804.
35. Ali, H., Gaël, C., Eric, L., Pierre, M., Rémi, D. The kinetic behavior of Liquid Silicone Rubber: A comparison between thermal and rheological approaches based on gel point determination, *React. Funct. Polym.*2016 (101), 20-27.
36. In-Kwon, H., Sangmook, L. Cure kinetics and modeling the reaction of silicone rubber, *J. Ind. Eng. Chem.* 2013 (19/1), 42-47.
37. Wong, L.S., Chandran, S.N., Rajasekar, R.R., Kong, S.Y. Pozzolanic characterization of waste newspaper ash as a supplementary cementing material of concrete cylinders. *Case Stud. Constr. Mater. 2022 (17),* e01342.
38. Rajput, D., Bhagade, S.S., Raut, S.P., Ralegaonkar, R.V., Mandavgane, S.A. Reuse of cotton and recycle paper mill waste as building material. *Constr Build Mater.* 2012 (34), 470-475.
39. Sales, D.C., Cabral, A.E., Medeiros, M.S. Development of fiberboard panels manufactured from reclaimed cement bags. *Constr Build Mater.* 2021 (34), 101525.
40. Ardanuy, M., Claramunt, Filho, R.D.T. Cellulosic fiber reinforced cement-based composites: A review of recent research. *Constr Build Mater*. 2015 (79), 115-128.